

# Scaling Properties of the Probability Distribution of Lattice Gribov Copies

A.Y. Lokhov<sup>a</sup>, O. Pène<sup>b</sup>, C. Roiesnel<sup>a</sup>

<sup>a</sup> Centre de Physique Théorique<sup>1</sup> de l'École polytechnique  
F91128 Palaiseau cedex, France

<sup>b</sup>Laboratoire de Physique Théorique et Hautes Energies<sup>2</sup>  
Université de Paris XI, Bâtiment 211, 91405 Orsay Cedex, France

## Abstract

We study the problem of the Landau gauge fixing in the case of the  $SU(2)$  lattice gauge theory. We show that the probability to find a lattice Gribov copy increases considerably when the physical size of the lattice exceeds some critical value  $\approx 2.75/\sqrt{\sigma}$ , almost independent of the lattice spacing. The impact of the choice of the copy on Green functions is presented. We confirm that the ghost propagator depends on the choice of the copy, this dependence decreasing for increasing volumes above the critical one. The gluon propagator as well as the gluonic three-point functions are insensitive to choice of the copy (within present statistical errors). Finally we show that gauge copies which have the same value of the minimisation functional ( $\int d^4x (A_\mu^a)^2$ ) are equivalent, up to a global gauge transformation, and yield the same Green functions.

CPHT-RR 065.1105  
LPT-Orsay/05-76

## 1 Introduction

The question of the quantisation in the infrared of a non-Abelian gauge theory is very important for the understanding of diverse non-perturbative phenomena. The main problem that arises while performing the quantisation in the covariant gauge is the problem of the non-uniqueness of the solution of the equation specifying the gauge-fixing condition, that was pointed out by Gribov [1]. In fact, the solution is unique for fields having small magnitude. A solution proposed in [1] consists in restricting the (functional) integration over gauge fields in the partition function to the region inside the so called Gribov horizon (the surface, closest to the trivial field  $\mathcal{A}_\mu = 0$ , on which the Faddeev-Popov determinant vanishes).

The Gribov's quantisation prescription is explicitly realised in the lattice formulation. Indeed, the procedure of Landau gauge fixing on the lattice (see [2] for a review) constraints all the eigenvalues of the Faddeev-Popov operator to be positive. Thus lattice

---

<sup>1</sup>Unité Mixte de Recherche 7644 du Centre National de la Recherche Scientifique

<sup>2</sup>Unité Mixte de Recherche 8627 du Centre National de la Recherche Scientifique

gauge configurations in Landau gauge are located inside the Gribov region, and all calculations on the lattice are done within the Gribov's quantisation prescription. But we also know that this is not enough - the gauge is not uniquely fixed even in this case, and there are secondary solutions (Gribov copies) inside the Gribov region ([3],[4]). The smaller region free of Gribov copies is called the fundamental modular region ([3],[5], [6]). On a finite lattice the gauge may be fixed in a unique way, but that reveals to be technically difficult (cf. the following section).

The quantities that are sensitive to the choice of the infrared quantisation prescription are Green functions. A lot of work regarding the influence of Gribov copies on lattice ghost and gluon propagators in the case of  $SU(2)$  and  $SU(3)$  gauge groups has already been done ([7],[8],[9],[10],[11],[12],[13]). Summarising the results, the infrared divergence of the ghost propagator is lessened when choosing Gribov copies closer to the fundamental modular region, and the gluon propagator remains the same (within today's statistical precision). In this paper we confirm these results in the case of the  $SU(2)$  gauge group, and present a study of the influence of Gribov copies on the three-gluon vertex in symmetric and asymmetric kinematic configurations. We also discuss in details the structure of minima of the gauge-fixing functional. The authors of [8] reported that the number of minima of the gauge-fixing functional decrease with the  $\beta$  parameter (the bare lattice coupling). We perform a thorough analysis of the volume dependence of this phenomenon. We define a probability to find a lattice Gribov copy, and our computation shows that this probability increases considerably when the physical size of the lattice exceeds some critical value, around  $2.75/\sqrt{\sigma}$ , where  $\sigma$  is the string tension.

## 2 Non-perturbative Landau gauge fixing on the lattice

A lattice gauge configuration  $U_{C_0}$  generated during the simulation process is not gauge-fixed. One has to perform a gauge transformation  $\{u(x)\}$  on it in order to move it along its gauge orbit up to the intersection with the surface  $f_L[U_\mu(x)] = 0$  specifying the Landau gauge-fixing condition. But there is no need to have an explicit form of  $\{u(x)\}$ . Instead we do an iterative minimisation process that starts at  $U_{C_0}$  and converges to the gauge fixed configuration  $U_C^{(u)}$ . Let us first illustrate it on the example of the Landau gauge in the continuum limit. For every gauge field  $\mathcal{A}$  one defines a functional

$$F_{\mathcal{A}}[u(x)] = -\text{Tr} \int d^4x \mathcal{A}_\mu^{(u)}(x) \mathcal{A}_\mu^{(u)}(x) = -\|\mathcal{A}^{(u)}\|^2, \quad u(x) \in SU(N_c). \quad (1)$$

Expanding it up to the second order around some group elements  $\{u_0(x)\}$  we have (writing  $u = e^X u_0$ ,  $X \in \mathfrak{su}(N_c)$ )

$$F_{\mathcal{A}}[u(x)] = F_{\mathcal{A}}[u_0(x)] + 2 \int d^4x \text{Tr} (X \partial_\mu \mathcal{A}_\mu^{(u_0)}) + \int d^4x \text{Tr} (X^\dagger \mathcal{M}_{\text{FP}} [\mathcal{A}^{(u_0)}] X) + \dots \quad (2)$$

Note that the quadratic form defining the second order derivatives is the Faddeev-Popov operator. Obviously, if  $u_0$  is a local minimum we have a double condition

$$\begin{cases} \partial_\mu \mathcal{A}_\mu^{(u_0)} = 0 \\ \mathcal{M}_{\text{FP}} [\mathcal{A}^{(u_0)}] \text{ is positive definite.} \end{cases} \quad (3)$$

Hence, the minimisation of the functional (1) allows not only to fix the Landau gauge, but also to obtain a gauge configuration inside the Gribov horizon (cf. Figure 1). On the

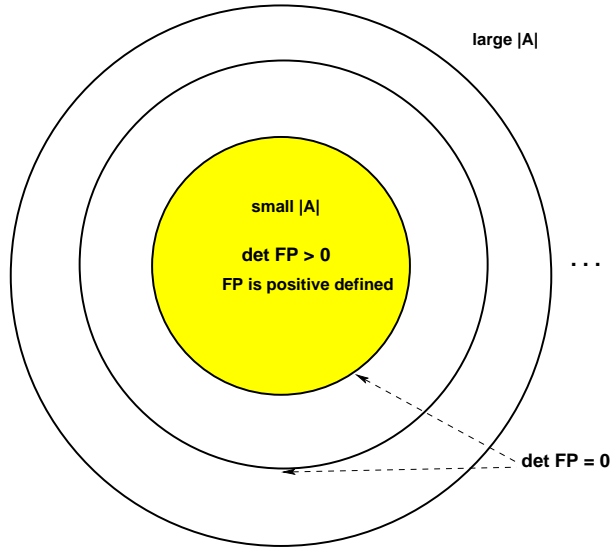


Figure 1: Restriction of the integration domain in the partition function to the Gribov region (hatched), and the Gribov horizon. “FP” is the Faddeev-Popov operator.

lattice, the discretised functional (1) reads

$$F_U[u] = -\frac{1}{V} \Re \epsilon \text{Tr} \sum_{x,\mu} u(x) U_\mu(x) u^\dagger(x + e_\mu), \quad (4)$$

where  $U_\mu(x)$  is the standard gauge link variable. Then at a local minimum  $u_0$  we have a discretised Landau gauge fixing condition

$$\sum_\mu \left( \mathcal{A}_\mu^{(u_0)} \left( x + \frac{e_\mu}{2} \right) - \mathcal{A}_\mu^{(u_0)} \left( x - \frac{e_\mu}{2} \right) \right) = 0. \quad (5)$$

that we write in a compact form  $\nabla_\mu \mathcal{A}_\mu^{(u_0)} = 0$ . Here

$$\mathcal{A}_\mu \left( x + \frac{e_\mu}{2} \right) = \frac{U_\mu(x) - U_\mu^\dagger(x)}{2}. \quad (6)$$

The second derivative (the equivalent of the second-order term in (2)) can be written as

$$\frac{d^2}{ds^2} F_U [u(s, x)] = -\frac{1}{V} (\omega, \nabla_\mu \mathcal{A}'_\mu) \quad (7)$$

where

$$\mathcal{A}'_\mu = \frac{1}{2} \left( -\omega(x) U_\mu^{(u)}(x) + U_\mu^{(u)}(x) \omega(x + e_\mu) + \omega(x + e_\mu) U_\mu^{(u)\dagger}(x) - U_\mu^{(u)\dagger}(x) \omega(x) \right). \quad (8)$$

This defines a quadratic form  $(\omega, \mathcal{M}_{FP}^{\text{lat}}[U] \omega)$  where the operator  $\mathcal{M}_{FP}^{\text{lat}}[U]$  is the lattice version of the Faddeev-Popov operator ([14]). It reads

$$\begin{aligned} \left( \mathcal{M}_{FP}^{\text{lat}}[U] \omega \right)^a(x) = & \frac{1}{V} \sum_\mu \left\{ S_\mu^{ab}(x) (\omega^b(x + e_\mu) - \omega^b(x)) - (x \leftrightarrow x - e_\mu) + \right. \\ & \left. + \frac{1}{2} f^{abc} \left[ \omega^b(x + e_\mu) A_\mu^c \left( x + \frac{e_\mu}{2} \right) - \omega^b(x - e_\mu) A_\mu^c \left( x - \frac{e_\mu}{2} \right) \right] \right\}, \quad (9) \end{aligned}$$

where

$$S_{\mu}^{ab}(x) = -\frac{1}{2}\text{Tr}(\{t^a, t^b\}(U_{\mu}(x) + U_{\mu}^{\dagger}(x))). \quad (10)$$

It is straightforward to check that in the continuum limit  $a \rightarrow 0$  one finds the familiar expression of the Faddeev-Popov operator.

For the Landau gauge fixing in our numerical simulation we have used the Overrelaxation algorithm with  $\omega = 1.72$ . We stop the iteration process of the minimising algorithm when the following triple condition is fulfilled:

$$\begin{aligned} \frac{1}{V(N_c^2 - 1)} \sum_{x,\mu} \text{Tr} \left[ (\nabla_{\mu} \mathcal{A}_{\mu}^{(u_0)}) (\nabla_{\mu} \mathcal{A}_{\mu}^{(u_0)})^{\dagger} \right] &\leq \Theta_{\max_x |\partial_{\mu} A_{\mu}^a|} = 10^{-18} \\ \frac{1}{V(N_c^2 - 1)} \left| \sum_x \text{Tr} [u^{(n)}(x) - \mathbb{I}] \right| &\leq \Theta_{\delta u} = 10^{-9} \\ \forall a, t_1, t_2 \quad \left| \frac{A_0^a(t_1) - A_0^a(t_2)}{A_0^a(t_1) + A_0^a(t_2)} \right| &\leq \Theta_{\delta A_0} = 10^{-7}. \end{aligned} \quad (11)$$

where  $u^{(n)}(x)$  is the matrix of the gauge transformation  $u(x)$  at the iteration step  $n$ , and the charge

$$A_0^a(\vec{x}, t) = \int d^3 \vec{x} A_0^a(\vec{x}, t) \quad (12)$$

must be independent of  $t$  in Landau gauge when periodical boundary conditions for the gauge field are used. The choice of numerical values for the stopping parameters is discussed at the end of the next section.

### 3 The landscape of minima of the functional $F_U$

The functional  $F_U$  (4) has a form similar to the energy of a spin glass. The last is known to possess a very large number of metastable states, i.e. spin configurations whose energy increases when any spin is reversed. Typically, the number of these states grows exponentially with the number of spins.

Let us consider the landscape of the functional  $F_U$ . One of its characteristics is the distribution of values at minima  $F_{\min}$  of  $F_U$ . We know that for small magnitudes of the gauge field all the link matrices  $U_{\mu}(x)$  (they play the role of couplings between the “spin” variables) are close to the identity matrix, and thus the minimum is unique. Their number increases when the bare lattice coupling  $\beta$  decreases, because the typical magnitude of the phase of  $U_{\mu}(x)$  grows in this case and thus link matrices move farther from the identity matrix. The number of minima also increases with the number of links (at fixed  $\beta$ ) because in this case there are more degrees of freedom in the system. At Figure 2 we present typical histograms of the distribution of  $F_{\min}$  for one given gauge configuration, as a function of the  $\beta$  parameter. We see that when  $\beta$  is large ( $\beta \gtrsim 2.5$  for the volume  $V = 8^4$  considered at Figure 2), we typically find only one value of  $F_{\min}$ . On the contrary, for very small values of  $\beta$  we find many different minima (cf. Figure 3). These values of  $\beta$  correspond to almost random links  $U_{\mu}(x)$ . In the following section we show that field configurations having the same  $F_{\min}$  are in fact equivalent up to a global gauge transformation.

The probability to find a secondary minimum depends on the value of the  $\beta$  parameter. We can calculate this probability in the following way. For each orbit we fix the gauge

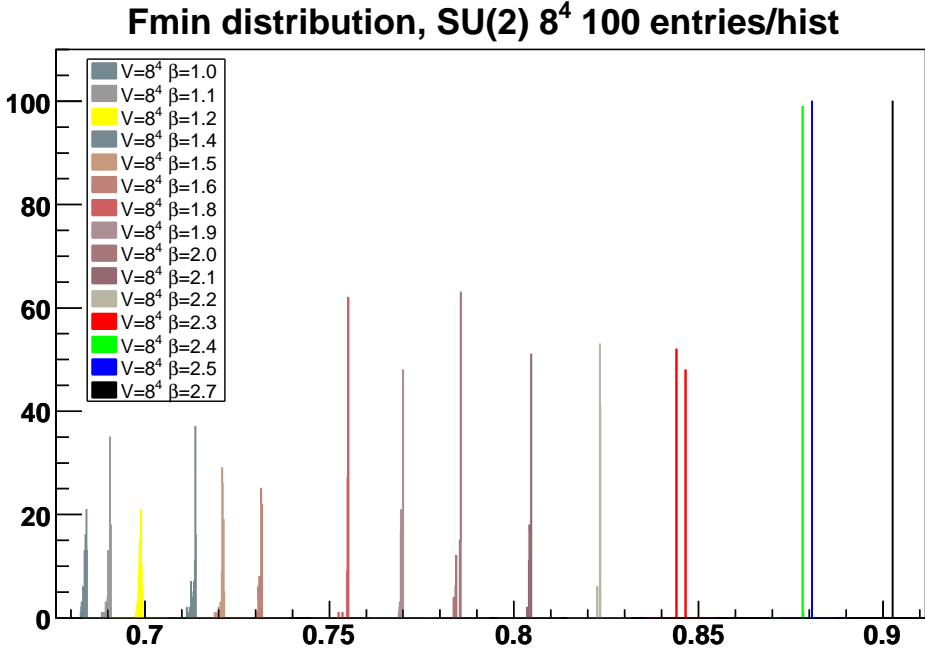


Figure 2: Histogram of minima values  $F_{\min}$  for different  $\beta$  for *one particular* gauge-field configuration,  $|\partial_\mu A_\mu^a(x)| \leq 10^{-9}$ . Here  $N_{\text{GF}} = 100$ . The histograms are ranged in the order the increase of the  $\beta$  parameter.

$N_{\text{GF}}$  times, each gauge fixing starts after a random gauge transformation of the initial field configuration. We thus obtain a distribution of minima  $F_{\min}$ . This distribution gives us the number of minima  $N(F^i)$  as a function of the value of  $F^i \equiv F_{\min}^i$ . The relative frequency of a minimum  $F^i$  is defined by

$$\omega_i = \frac{N(F^i)}{\sum_i N(F^i)}, \quad (13)$$

where  $\sum_i N(F^i) = N_{\text{GF}}$ . Then the weighted mean number of copies per value of  $F_{\min}$  is given by

$$\bar{N} = \sum_i \omega_i N(F^i). \quad (14)$$

This allows us to define a probability to find a secondary minimum when fixing the Landau gauge for a gauge field configuration :

$$p_{1\text{conf}} = 1 - \frac{\bar{N}}{\sum_i N(F^i)}. \quad (15)$$

If one finds the same value of  $F_{\min}$  for all  $N_{\text{GF}}$  tries then this probability is zero. On the contrary, if all  $F_i$  are different then  $p$  is close to one.

Having the probability to find a secondary minimum when fixing the gauge for *one particular* configuration we can calculate the Monte-Carlo *average*  $\langle \star \rangle$  on gauge orbits, i.e. on “spin couplings”  $U_\mu(x)$ . We obtain finally the overall probability to find a secondary minimum during a numerical simulation:

$$P(\beta) \equiv \langle p_{1\text{conf}} \rangle = 1 - \left\langle \frac{\bar{N}}{\sum_i N(F^i)} \right\rangle. \quad (16)$$

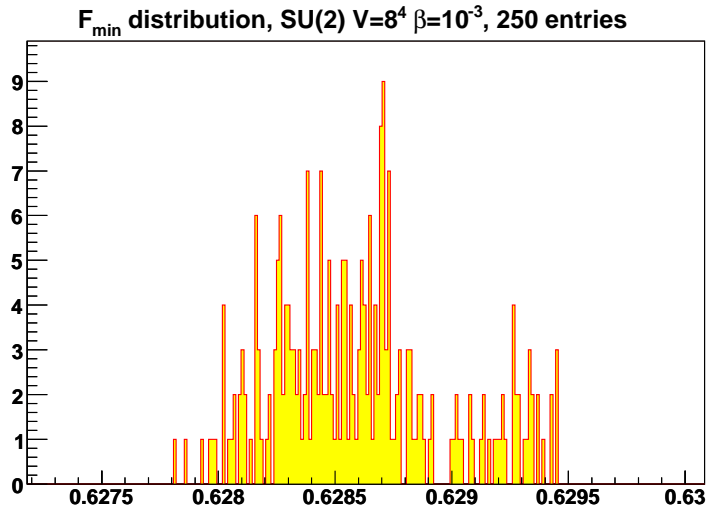


Figure 3: Histogram of minima values  $F_{\min}$  for very a small value of  $\beta = 10^{-3}$ ,  $|\partial_\mu A_\mu^a(x)| \leq 10^{-9}$ .

We have performed simulations in the case of  $SU(2)$  lattice gauge theory at volumes  $V = \{8^4, 10^4, 12^4, 16^4\}$  for  $\beta$  varying from 1.4 to 2.9. For each value of  $\beta$  we generated 100 independent Monte-Carlo gauge configurations, and we fixed the gauge  $N_{\text{GF}} = 100$  times for every configuration. Between each gauge fixing a random gauge transformation of the initial gauge configuration was performed, and the minimising algorithm stops when the triple condition (11) is satisfied. The resulting probability to find a secondary minimum is presented at (Figures 4-7).

As expected, the probability is small when  $\beta$  is large, and it is close to one when  $\beta$  is small. The dispersion was calculated using the Jackknife method. The physical meaning of this dispersion is the following: when the error is small, all gauge configurations have a similar number of secondary minima. On the contrary, this dispersion is large if there are some exceptional gauge configurations having a different number of copies. At small  $\beta$  almost all gauge configurations have many secondary minima, that is why the dispersion of the probability is small. At large  $\beta$  almost all gauge configurations have a unique minimum, but some of them can have copies. This may considerably increase the dispersion of the probability. The appearance of exceptional gauge configuration possessing a large density of close-to-zero eigenvalues of the Faddeev-Popov operator has been recently reported [13]. Probably these fields are related with those having a lot of secondary minima at large  $\beta$ 's, and this correlation deserves a separate study.

We can fit the data from Figures 4-7 with an empirical formula

$$P(\beta) = \frac{A}{1 + e^{B(\beta - \beta_c)}} \quad (17)$$

in order to define a characteristic coupling  $\beta_c$  when the probability to find a copy decreases considerably. One can define  $\beta_c$  as corresponding to the semi-heights of the probability function  $P(\beta)$ . At this value of  $\beta$  an *equally probable* secondary attractor of the functional  $F_U$  appears. The fit has been performed for the points between dashed lines at Figures 4-7, and the results for the fit parameters are given ibidem and in Table 1. We see that  $\beta_c$  depends on the volume of the lattice. Let us check whether these values correspond to some physical scale. According to works [15],[16] one has the following expression for the

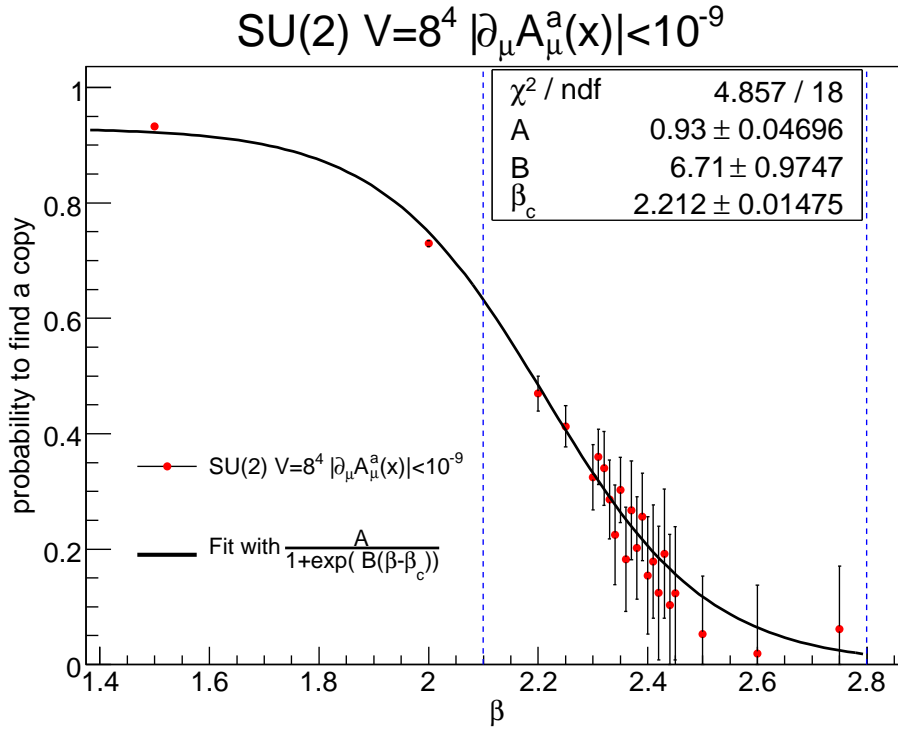


Figure 4: Probability (averaged over gauge orbits) to find a secondary minimum as a function of  $\beta$  at volume  $V = 8^4$ .

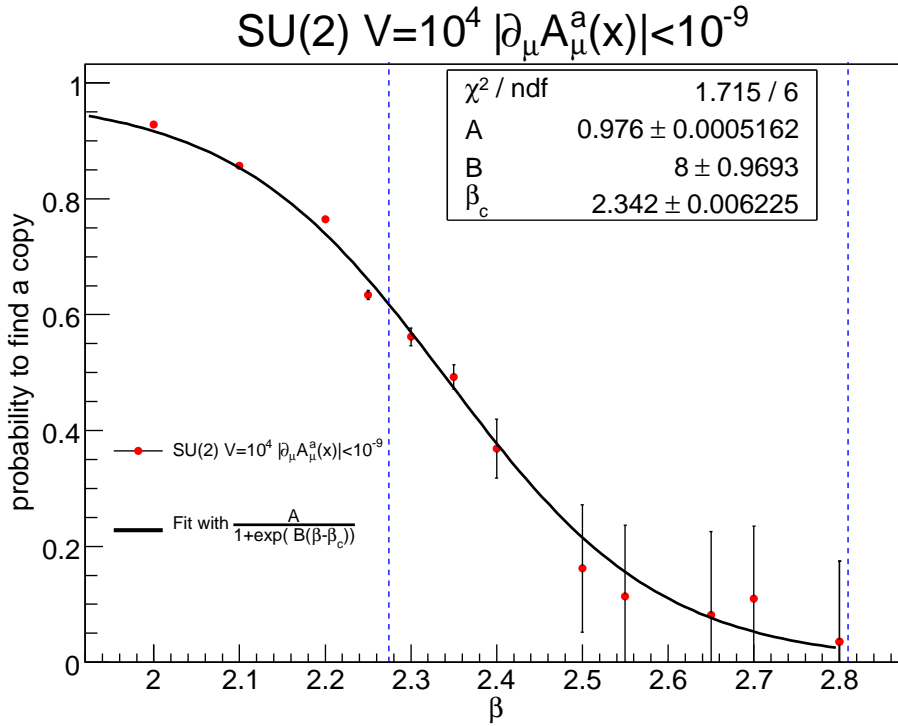


Figure 5: Probability (averaged over gauge orbits) to find a secondary minimum as a function of  $\beta$  at volume  $V = 10^4$ .

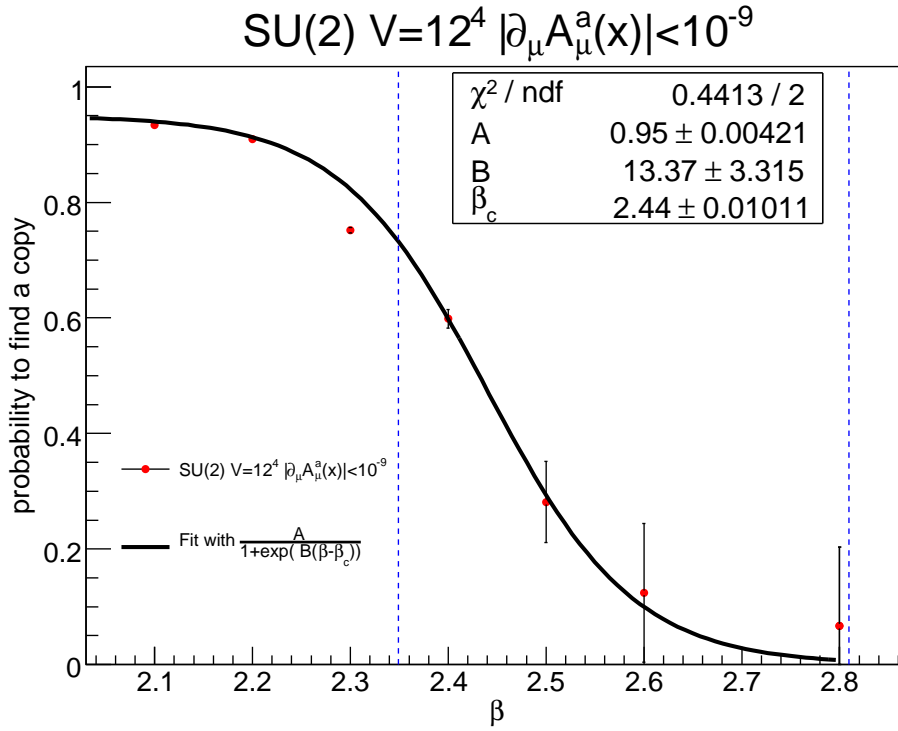


Figure 6: Probability (averaged over gauge orbits) to find a secondary minimum as a function of  $\beta$  at volume  $V = 12^4$ .

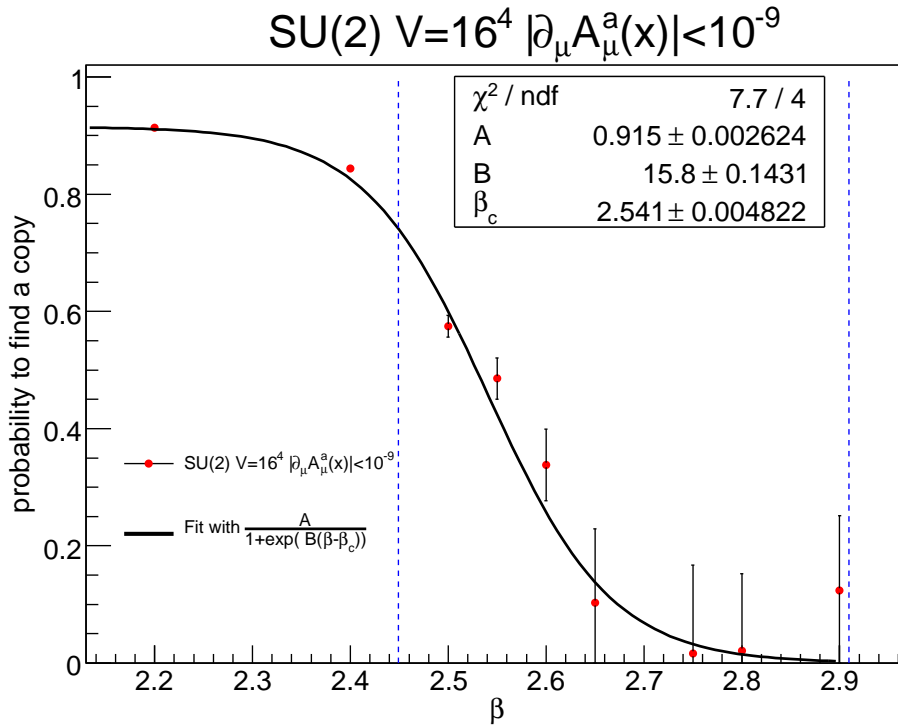


Figure 7: Probability (averaged over gauge orbits) to find a secondary minimum as a function of  $\beta$  at volume  $V = 16^4$ .



string tension  $\sigma$  for  $\beta \geq 2.3$ :

$$[\sigma a^2](\beta) \simeq e^{-\frac{4\pi^2}{\beta_0}\beta + \frac{2\beta_1}{\beta_0^2} \log\left(\frac{4\pi^2}{\beta_0}\beta\right) + \frac{4\pi^2}{\beta_0} \frac{d}{\beta} + c} \quad (18)$$

with  $c = 4.38(9)$  and  $d = 1.66(4)$ . Using this formula, we define a characteristic scale corresponding to the critical values  $\beta_c$  from (Figures 4-7) :

$$\lambda_c = a(\beta_c) \cdot L$$

in the string tension units,  $L$  is the length of the lattice. In the last column of Table 1 we summarise the results. We see that for the values of  $\beta_c$  in the scaling regime when the

$L$	$\beta_c$	$\chi^2/\text{ndf}$	$\lambda_c$ , in units of $1/\sqrt{\sigma}$
8	2.221(14)	0.27	3.85(31)
10	2.342(6)	0.28	3.20(21)
12	2.44(1)	0.22	2.78(20)
16	2.541(5)	1.92	2.68(17)

Table 1: The characteristic length defining the appearance of secondary minima. The errors for  $\lambda_c$  include errors for  $d$  and  $c$  parameters, and the fitted error for  $\beta_c$

formula (18) is applicable ( $\beta \geq 2.3$ ) we obtain compatible values for the physical length  $\lambda_c$ .

This suggests that lattice Gribov copies appear when the physical size of the lattice exceeds a critical value of around  $2.75/\sqrt{\sigma}$ . At first approximation  $\lambda_c$  is scale invariant, but a slight dependence in the lattice spacing remains.

In principle, the parameter  $\beta_c$  can be calculated with good precision. One should do it in the case of  $SU(3)$  gauge group, because the dependence of the lattice spacing on the bare coupling is softer, and the scaling of the theory has been better studied than in the case of the  $SU(2)$  theory.

Let us discuss the dependence of above results on the choice of the stopping parameters (11). In the Table 6 we present the probabilities  $P(2.0), P(2.3), P(2.8)$ , calculated on a  $8^4$  lattice with different values of the parameters (11). One can see that our choice of stopping parameters in (11) is strict enough to ensure the independence of our results on the further increase of the parameter  $\Theta_{\max_x |\partial_\mu A_\mu^a|}$ .

## 4 Green functions and the lattice Gribov copies

### 4.1 Two- and three-point lattice Green functions

Lattice Green functions are computed as Monte-Carlo averages over gauge-fixed gluon field configurations.

Gluonic Green functions are defined using the definition (6) of the gauge field. The ghost propagator  $F^{(2)ab}(x-y)$  is computed, with the algorithm given in [17], by numerical inversion of the Faddeev-Popov operator (9), e.g.

$$F^{(2)}(x-y)\delta^{ab} \equiv \left\langle \left( \mathcal{M}_{FP}^{\text{lat}}{}^{-1}[A] \right)_{xy}^{ab} \right\rangle. \quad (19)$$

The gluon propagator in Landau gauge may be parametrised as

$$G_{\mu\nu}^{(2)ab}(p, -p) \equiv \left\langle \tilde{A}_\mu^a(-p) \tilde{A}_\nu^b(p) \right\rangle = \delta^{ab} \left( \delta_{\mu\nu} - \frac{p_\mu p_\nu}{p^2} \right) G^{(2)}(p^2) \quad (20)$$

completed with

$$G_{\mu\nu}^{(2)ab}(0, 0) = \delta^{ab} \delta_{\mu\nu} G^{(2)}(0). \quad (21)$$

The ghost propagator is parametrised in the usual way:

$$\tilde{F}^{(2)ab}(p, -p) \equiv \left\langle \tilde{c}^a(-p) \tilde{c}^b(p) \right\rangle = \delta^{ab} F^{(2)}(p^2) \quad (22)$$

The coupling constant can be defined non-perturbatively by the amputation of a three-point Green-functions from its external propagators. But this requires to fix the kinematic configuration of the three-point Green-function at the normalisation point. On the lattice one usually uses either a fully symmetric kinematic configuration (denoted MOM) or a zero point kinematic configuration with one vanishing external momentum (denoted generically  $\widetilde{\text{MOM}}$ ). In what follows we only speak about gluonic three-point functions.

### Symmetric case

There are only two independent tensors in Landau gauge in the case of the symmetric three-gluon Green function [18]:

$$\mathcal{T}_{\mu_1, \mu_2, \mu_3}^{[1]}(p_1, p_2, p_3) = \delta_{\mu_1 \mu_2} (p_1 - p_2)_{\mu_3} + \delta_{\mu_2 \mu_3} (p_2 - p_3)_{\mu_1} + \delta_{\mu_3 \mu_1} (p_3 - p_1)_{\mu_2} \quad (23)$$

$$\mathcal{T}_{\mu_1, \mu_2, \mu_3}^{[2]}(p_1, p_2, p_3) = \frac{(p_1 - p_2)_{\mu_3} (p_2 - p_3)_{\mu_1} (p_3 - p_1)_{\mu_2}}{p^2}. \quad (24)$$

Then the three-gluon Green function in the MOM scheme ( $p_1^2 = p_2^2 = p_3^2 = \mu^2$ ) can be parametrised as

$$\begin{aligned} \left\langle \tilde{A}_{\mu_1}^a(p_1) \tilde{A}_{\mu_2}^b(p_2) \tilde{A}_{\mu_3}^c(p_3) \right\rangle &= f^{abc} \left[ G^{(3)\text{sym}}(\mu^2) \mathcal{T}_{\mu'_1, \mu'_2, \mu'_3}^{[1]}(p_1, p_2, p_3) \prod_{i=1,3} \left( \delta_{\mu'_i \mu_i} - \frac{p_{i\mu'_i} p_{i\mu_i}}{\mu^2} \right) + \right. \\ &\quad \left. + H^{(3)}(\mu^2) \mathcal{T}_{\mu_1, \mu_2, \mu_3}^{[2]}(p_1, p_2, p_3) \right] \end{aligned} \quad (25)$$

The scalar function  $G^{(3)\text{sym}}(\mu^2)$ , proportional to the coupling  $g_0$  at tree level, may be extracted by the following projection:

$$\begin{aligned} G^{(3)\text{sym}}(\mu^2) &= \left( \mathcal{T}_{\mu'_1, \mu'_2, \mu'_3}^{[1]}(p_1, p_2, p_3) \prod_{i=1,3} \left( \delta_{\mu'_i \mu_i} - \frac{p_{i\mu'_i} p_{i\mu_i}}{\mu^2} \right) + \frac{1}{2} \mathcal{T}_{\mu'_1, \mu'_2, \mu'_3}^{[2]}(p_1, p_2, p_3) \right) \times \\ &\quad \times \frac{1}{18\mu^2} \frac{f^{abc}}{N_c(N_c^2 - 1)} \left\langle \tilde{A}_{\mu_1}^a(p_1) \tilde{A}_{\mu_2}^b(p_2) \tilde{A}_{\mu_3}^c(p_3) \right\rangle. \end{aligned} \quad (26)$$

## Asymmetric case

The three-gluon Green function with one vanishing external propagator ([19],[18]) can be parametrised as

$$G_{\mu\nu\rho}^{(3)abc}(p, 0, -p) \equiv \left\langle \tilde{A}_\mu^a(-p) \tilde{A}_\nu^b(p) \tilde{A}_\rho^c(0) \right\rangle = 2f^{abc} p_\rho \left( \delta_{\mu\nu} - \frac{p_\mu p_\nu}{p^2} \right) G^{(3)\text{asym}}(p^2), \quad (27)$$

and thus

$$G^{(3)\text{asym}}(p^2) = \frac{1}{6p^2} \frac{f^{abc}}{N_c(N_c^2 - 1)} \delta_{\mu\nu} p_\rho G_{\mu\nu\rho}^{(3)abc}(p, 0, -p). \quad (28)$$

## Gauge coupling

Using the scalar functions  $G^{(2)}$  and  $G^{(3)}$  (the last stands for  $G^{(3)\text{asym}}$  or  $G^{(3)\text{sym}}$ ), the gauge coupling at the renormalisation scale  $\mu^2$  is defined by

$$g_R(\mu^2) = \frac{G^{(3)}(p_1^2, p_2^2, p_3^2)}{G^{(2)}(p_1^2) G^{(2)}(p_2^2) G^{(2)}(p_3^2)} Z_3^{3/2}(\mu^2) \quad (29)$$

in the case of three-gluon vertices, where the choice of  $p_i$  determines the renormalisation scheme ( $\overline{\text{MOM}}$  or  $\text{MOM}$ ). In paper [20] it is shown that in the  $\overline{\text{MOM}}$  schemes  $g_R(\mu^2)$  vanishes in the zero momentum limit. It is interesting to investigate the possible influence of Gribov copies on this behaviour. We address this question in the following section.

## 4.2 Influence of the lattice gauge fixing

A natural question that arises after the study of the distribution of  $F_{\min}$  is whether the gauge configurations having the same value of  $F_{\min}$  are equivalent, i.e. they differ only by a global gauge transformation.

This can be checked by calculating the two-point gluonic correlation function on the gauge configuration. Indeed, according to the lattice definition of the gauge field that we used (6),

$$G_{1\text{ conf}}^{(2)}(x - y) \propto \text{Tr} \left[ (U_\mu(x) - U_\mu^\dagger(x)) \cdot (U_\nu(y) - U_\nu^\dagger(y)) \right]. \quad (30)$$

Applying a global gauge transformation  $U_\mu(x) \rightarrow V U_\mu(x) V^\dagger$  we see that the gluon propagator remains unchanged. This is also the case of the ghost propagator scalar function. We have checked numerically that the values of the gluon and the ghost propagators in Fourier space are the same for gauge configurations having the same  $F_{\min}$  (cf. Tables 2,3). For comparison, the data from a lattice Gribov copy (the same gauge configuration but having different value of  $F_{\min}$ ) is also given. We see that the values are almost the same for gauge configurations having the same  $F_{\min}$  contrarily to those coming from different minima. In fact, taking in account rounding errors appearing during the calculation, we may say that gauge configurations having the same  $F_{\min}$  are equivalent.

The second question that has already been considered by ([7],[8],[9],[10],[11],[12],[13]) is the dependence of Green functions on the choice of the minimum. For this purpose we have performed the following simulation: for every of the 100 gauge configurations used to compute Green functions the gauge was fixed 100 times, and the Monte-Carlo average was computed with respect to the “first copy” (fc) found by the minimisation algorithm and the “best copy” (bc), having the smallest value of  $F_{\min}$ . We have calculated the gluon and the ghost propagators, and also the three-gluon Green functions in symmetric and

$F_{\min}$	-0.871010810260	-0.871010810260	-0.870645877060
$V \cdot G^{(2)}(p^2) : p^2 = 0$	4249297	4249295	3322788
$p^2 = 1$	2012518	2012516	2006186
$p^2 = 2$	1215762	1215762	1362671
$p^2 = 3$	834876.3	834876.4	798032
$p^2 = 4$ $p^{[4]}=16$	620065.2	620067.3	434235.6
$p^2 = 4$ $p^{[4]}=4$	521585.0	521585.2	556509.6
$p^2 = 5$	410698.8	410698.5	440623.9

Table 2: Gluon correlator calculated on different gauge configurations having the same value of  $F_{\min}$  (columns 2 and 3), compared to values from the "secondary" minimum (column 4). We present data for all  $H_4$  group orbits for the momentum  $p^2 = 4$  ([21],[17]). Notice that in all this paper the momenta are given in units of  $2\pi/(aL)$ . Simulation has been performed with parameters  $V = 16^4, \beta = 2.4$

$F_{\min}$	-0.871010810260	-0.871010810260	-0.870645877060
$F^{(2)}(p^2) p^2 = 1$	14.06473	14.06473	14.82984
$p^2 = 2$	6.278253	6.278253	6.736338
$p^2 = 3$	3.757531	3.757531	3.939130
$p^2 = 4$ $p^{[4]}=16$	2.929602	2.929602	2.705556
$p^2 = 4$ $p^{[4]}=4$	2.599088	2.599088	2.775566
$p^2 = 5$	2.071200	2.071200	2.011100

Table 3: Ghost correlator calculated on different gauge configurations having the same value of  $F_{\min}$  (columns 2 and 3), compared to values from the "secondary" minimum (column 4). We present data for all  $H_4$  group orbits for the momentum  $p^2 = 4$  ([21],[17]). Simulation has been performed with parameters  $V = 16^4, \beta = 2.4$

$\beta$	$L$	$p^2$	$F_{\text{fc}}^{(2)}(p^2) - F_{\text{bc}}^{(2)}(p^2)$	$\frac{F_{\text{fc}}^{(2)}(p^2) - F_{\text{bc}}^{(2)}(p^2)}{F_{\text{bc}}^{(2)}(p^2)}$
2.1	8	1	0.211	0.045
2.1	16	4 $p^{[4]}=16$	0.145	0.033
2.2	8	1	0.078	0.019
2.2	16	4 $p^{[4]}=16$	0.023	0.006
2.3	8	1	0.086	0.024
2.3	16	4 $p^{[4]}=16$	0.114	0.034

Table 4: Volume dependence of the ghost propagators, from Tables 7- 26

asymmetric kinematic configurations. The simulations have been performed on lattices of volumes  $8^4$  and  $16^4$  for  $\beta = 2.1, 2.2, 2.3$ . At these values of  $\beta$  we are sure to have lattice Gribov copies. The results are given in Tables 7-29. All data is given in lattice units. We present data for all  $H_4$  group orbits ([21],[17]) for considered momenta, and we have checked that our results for two-point Green functions are consistent with numerical values given in [7],[8]. We conclude from Tables 7-29 that the ghost propagator is quite sensitive to the choice of the minimum - in the case of (bc) the infrared divergence is lessened. No systematic effect could be found for gluonic two- and three-point Green functions, the values in the cases of (fc) and (bc) being compatible within the statistical errors.

It is conjectured in [22] that in the infinite volume limit the expectation values calculated by integration over the Gribov region and the fundamental modular region become equal. However, the ghost propagator depends on this choice, even for volumes larger than the critical volume defined in section 3, see Table 19 where there is a four  $\sigma$  discrepancy for  $p^2 = 1$ . This dependence has been found to decrease slowly with the volume [12]. The results of section 3 indicate that the convergence can only happen beyond the critical size.

$\beta$	$L$	$\overline{\langle F_{\min} \rangle}_{\{U\}}$	$\delta \overline{\langle F_{\min} \rangle}_{\{U\}}$
2.2	8	-0.8236	0.003744
	10	-0.8262	0.002367
	12	-0.8272	0.001377
	16	-0.8279	0.000802
2.4	8	-0.8642	0.005270
	12	-0.8669	0.002739
	12	-0.8686	0.001849
	16	-0.8702	0.001003

Table 5: Volume dependence of the Monte-Carlo+gauge orbit mean value at minima  $F_{\min}$  and the dispersion of this mean.

To check this we compare the fc-bc values of the ghost propagator, at one physical value of the momentum, for the orbit  $p^2 = 1$  on a  $8^4$  lattice and the orbit  $p^2 = 4, p^{[4]} = 16$  on the  $16^4$  lattice <sup>3</sup> at the same  $\beta$  (see Table 4). It happens indeed that the decrease is observed only at  $\beta = 2.1$  and  $2.2$ , in accordance with Table 1. However, these values of  $\beta$  are not in the scaling regime, and thus a study on larger lattices would be welcome. It is not surprising that the ghost propagator depends on the bc/fc choice: the bc corresponds to the fields further from the Gribov horizon where the Faddeev-Popov operator has a zero mode, whence the inverse Faddeev-Popov operator (ghost propagator) is expected to be smaller as observed. The correlation between the bc/fc choice and the gluon propagator is not so direct. Another quantity is obviously strongly correlated to the bc/fc choice: the value of  $F_{\min}$ . We tested the volume dependence of the Monte-Carlo+gauge orbit mean value of the quantity  $F_{\min}$  (see Tab.5). According to the argument given in [22], all minima become degenerate in the infinite volume limit, and closer to the absolute minimum (in the fundamental modular region). We see from the Table 5 that their average value and dispersion decrease with the volume at fixed  $\beta$ , in agreement with [22].

## 5 Conclusions

Our study showed that

- Lattice Gribov copies appear and their number grows very fast when the physical size of the lattice exceeds some critical value  $\approx 2.75/\sqrt{\sigma}$ . This result is fairly independent of the lattice spacing.
- The configurations lying on the same gauge orbit and having the same  $F_{\min}$  are equivalent, up to a global gauge transformation, and yield the same Green functions. Those corresponding to minima of  $F_U$  with different values of  $F_{\min}$  differ by a non-trivial gauge transformation, and thus they are not equivalent.
- We confirm the result ([7],[8],[9],[10],[11],[12],[13]) that the divergence of the ghost propagator is lessened when choosing the “best copy” (corresponding to the choice of the gauge configuration having the smallest value of  $F_U$ ). We also showed that gluonic Green functions calculated in the “first copy” and “best copy” schemes are compatible within the statistical error, no systematic effect was found. We conclude that gauge couplings that are defined by amputating the three-gluon vertices only

---

<sup>3</sup>Remember that the momentum in physical units is equal to  $2\pi p/(La)$  in our notations.

slightly depend on the choice of the minimum of  $F_U$ . It implies that the infrared behaviour of  $g_R(\mu^2)$  reported in [20] is not significantly influenced by lattice Gribov copies.

- We found that the influence of Gribov copies on the ghost propagator decreases with the volume when the physical lattice size is larger than the critical length discussed above. We also show that the quantity  $F_{\min}$  decreases when the volume increases. These two points are in agreement with the argument on the equality of the averages over the Gribov's region and the fundamental modular region [22].

The fact that the abundance of lattice Gribov copies is mainly an increasing function of the physical size of the lattice is not too surprising. The existence of Gribov copies is a non-perturbative phenomenon and as such is related [1] to the infrared properties of the Faddeev-Popov operator and to the confinement scale. It should then dominantly depend on the infrared cut-off, the size (or volume) of the lattice in physical units. A milder dependence on the ultraviolet cut-off, the lattice spacing, is also expected but the limited accuracy concerning the lattice spacing did not allow us to identify it. In a recent paper [13] the lowest eigenvalues of the Faddeev-Popov operator have been computed. A dependence on the size of the lattice is seen. A detailed study of this dependence in connection with our findings in this paper would be useful.

More generally, the question of extracting from lattice simulations informations about Gribov copies in the continuum limit is not a simple issue. However, bulk quantities, such as the one we propose in this paper, may be traced down to the continuum limit and provide precious information about continuum Gribov copies. The total number of lattice Gribov copies in a given gauge orbit may be large. All the minima of the functional  $F_{\mathcal{A}}[u(x)]$  (1) are possible end-points of the Landau gauge fixing algorithm, but their probability to be selected by the algorithm depends on the size of their domain of attraction and might vary significantly. This probability is therefore expected to depend on the attractor pattern and not on the choice of algorithm, which should be checked.

The explosion of the number of Gribov copies at larger volume does not contradict the statement that they have decreasing influence on expectation values [22]. Even more, this influence decreases when the number of Gribov copies is large enough (cf. Tables 4,1), i.e. above the critical volume that we have outlined.

We wish to continue this research in a few directions: more refined quantities may be defined, a better accuracy is needed, larger volumes studied, in particular to check if the ghost propagator dependence on the bc/fc choice fades away in the scaling regime. An extension of the study to  $SU(3)$  and to unquenched gauge configurations will be welcome.

**Note added in proof** While this paper was being submitted, a preprint has appeared [23] which adds to the gauge group the extra global symmetry of the quenched lattice action with respect to the centre of the gauge group. This leads to an extension of the notion of Gribov copies and it results a sensitivity of the gluon propagator upon the latter. We note that the copy dependence is mainly observed at small lattice volumes, below the critical size found by us.

$\beta$	$\Theta_{\max_x  \partial_\mu A_\mu^a }$	$\Theta_{A_0}$	$\Theta_{\delta u}$	$P(\beta)$	$\delta P(\beta)$	$\langle F_{\min} \rangle$	$\delta_{\text{RMS}} F_{\min}$
2.0	$10^{-10}$	$10^{-5}$	$10^{-5}$	0.729620	0.004738	0.78416564213526	0.00260692007045
2.0	$10^{-14}$	$10^{-5}$	$10^{-9}$	0.729606	0.004984	0.78416564421249	0.00260692062016
2.0	$10^{-14}$	$10^{-7}$	$10^{-9}$	0.729606	0.004985	0.78416564421259	0.00260692061867
→ 2.0	$10^{-18}$	$10^{-7}$	$10^{-9}$	0.729606	0.004985	0.78416564421258	0.00260692062307
2.0	$10^{-24}$	$10^{-7}$	$10^{-9}$	0.729606	0.004985	0.78416564421258	0.00260692062150
2.0	$10^{-28}$	$10^{-7}$	$10^{-9}$	0.729606	0.004985	0.78416564421258	0.00260692062134
2.3	$10^{-10}$	$10^{-5}$	$10^{-5}$	0.324636	0.056660	0.84466892598808	0.00415444722060
2.3	$10^{-14}$	$10^{-5}$	$10^{-9}$	0.324636	0.056660	0.84466892602737	0.00415444721015
2.3	$10^{-14}$	$10^{-7}$	$10^{-9}$	0.324636	0.056660	0.84466892602833	0.00415444720619
→ 2.3	$10^{-18}$	$10^{-7}$	$10^{-9}$	0.324636	0.056660	0.84466892602843	0.00415444720513
2.3	$10^{-24}$	$10^{-7}$	$10^{-9}$	0.324636	0.056660	0.84466892602847	0.00415444720356
2.3	$10^{-28}$	$10^{-7}$	$10^{-9}$	0.324636	0.056660	0.84466892602847	0.00415444720356
2.8	$10^{-10}$	$10^{-5}$	$10^{-5}$	0.024946	0.155566	0.89393978935534	0.00777035608940
2.8	$10^{-14}$	$10^{-5}$	$10^{-9}$	0.024946	0.155567	0.89393978936422	0.00777035609273
2.8	$10^{-14}$	$10^{-7}$	$10^{-9}$	0.024946	0.155567	0.89393978936434	0.00777035609111
→ 2.8	$10^{-18}$	$10^{-7}$	$10^{-9}$	0.024946	0.155567	0.89393978936448	0.00777035608963
2.8	$10^{-24}$	$10^{-7}$	$10^{-9}$	0.024946	0.155567	0.89393978936449	0.00777035608962
2.8	$10^{-28}$	$10^{-7}$	$10^{-9}$	0.024946	0.155567	0.89393978936449	0.00777035608962

Table 6: The influence of different stopping parameters (11) on the value of the probability  $P(\beta)$ . Simulations done for the lattice size  $V = 8^4$ , 100 Monte-Carlo configurations (we uses the same set of configurations for every value of  $\beta$ )  $\times N_{\text{NF}} = 100$  gauge fixings. The last two columns give the average value of  $F_{\min}$  and the standard dispersion of this average. The arrow indicates our choice of stopping parameters (11).

$SU(2)$ ,  $V = 8^4$  and  $\beta = 2.1$ , 100 Monte-Carlo configurations  $\times$  100 gauge fixings

Two point functions

$p^2$	$F_{fc}^{(2)}(p^2)$	$\delta F_{fc}^{(2)}(p^2)$	$F_{bc}^{(2)}(p^2)$	$\delta F_{bc}^{(2)}(p^2)$
1	4.898	0.099	4.687	0.071
2	2.046	0.039	1.959	0.043
3	1.210	0.021	1.168	0.023
4 $p^{[4]=16}$	0.961	0.023	0.925	0.021
4 $p^{[4]=4}$	0.834	0.019	0.801	0.013
5	0.696	0.007	0.680	0.014

Table 7: Ghost propagator,  $V = 8^4$   $\beta = 2.1$

$p^2$	$G_{fc}^{(2)}(p^2)$	$\delta G_{fc}^{(2)}(p^2)$	$G_{bc}^{(2)}(p^2)$	$\delta G_{bc}^{(2)}(p^2)$
0	11.161	0.438	10.894	0.418
1	6.225	0.129	6.248	0.135
2	4.089	0.035	4.095	0.043
3	2.883	0.033	2.868	0.023
4 $p^{[4]=16}$	2.329	0.043	2.305	0.031
4 $p^{[4]=4}$	2.129	0.023	2.147	0.015
5	1.773	0.009	1.785	0.008

Table 8: Gluon propagator,  $V = 8^4$   $\beta = 2.1$

Three point functions

$p^2$	$G_{fc}^{(3)asym}(p^2)$	$\delta G_{fc}^{(3)asym}(p^2)$	$G_{bc}^{(3)asym}(p^2)$	$\delta G_{bc}^{(3)asym}(p^2)$
1	29.636	2.081	29.408	2.721
2	19.018	1.168	18.387	1.173
3	11.513	0.971	12.293	1.739
4 $p^{[4]=16}$	10.424	0.857	11.817	1.126
4 $p^{[4]=4}$	6.968	0.618	6.547101	0.471
5	5.164	0.264	4.697285	0.293

Table 9: Three-gluon vertex in asymmetric kinematic configuration,  $V = 8^4$   $\beta = 2.1$

$p^2$	$G_{fc}^{(3)sym}(p^2)$	$\delta G_{fc}^{(3)sym}(p^2)$	$G_{bc}^{(3)sym}(p^2)$	$\delta G_{bc}^{(3)sym}(p^2)$
2	13.613	0.745	14.188	0.752
4	2.680	0.272	2.612	0.272

Table 10: Three-gluon vertex in symmetric kinematic configuration,  $V = 8^4$   $\beta = 2.1$



$SU(2)$ ,  $V = 8^4$  and  $\beta = 2.2$ , 100 Monte-Carlo configurations  $\times$  100 gauge fixings

Two point functions

$p^2$	$F_{fc}^{(2)}(p^2)$	$\delta F_{fc}^{(2)}(p^2)$	$F_{bc}^{(2)}(p^2)$	$\delta F_{bc}^{(2)}(p^2)$
1	4.178	0.103	4.100	0.070
2	1.749	0.045	1.735	0.037
3	1.042	0.027	1.032	0.024
4 $p^{[4]}=16$	0.835	0.030	0.821	0.024
4 $p^{[4]}=4$	0.720	0.016	0.715	0.014
5	0.614	0.017	0.609	0.014

Table 11: Ghost propagator,  $V = 8^4$   $\beta = 2.2$

$p^2$	$G_{fc}^{(2)}(p^2)$	$\delta G_{fc}^{(2)}(p^2)$	$G_{bc}^{(2)}(p^2)$	$\delta G_{bc}^{(2)}(p^2)$
0	20.170	0.620	20.241	0.665
1	8.359	0.129	8.247	0.122
2	4.431	0.039	4.433	0.037
3	2.870	0.028	2.857	0.025
4 $p^{[4]}=16$	2.111	0.038	2.153	0.041
4 $p^{[4]}=4$	2.021	0.013	2.038	0.019
5	1.642	0.014	1.652	0.013

Table 12: Gluon propagator,  $V = 8^4$   $\beta = 2.2$

Three point functions

$p^2$	$G_{fc}^{(3)asym}(p^2)$	$\delta G_{fc}^{(3)asym}(p^2)$	$G_{bc}^{(3)asym}(p^2)$	$\delta G_{bc}^{(3)asym}(p^2)$
1	78.913	4.405	81.523	5.131
2	36.170	1.393	35.784	1.809
3	17.851	2.147	18.475	1.860
4 $p^{[4]}=16$	20.516	1.064	20.621	1.115
4 $p^{[4]}=4$	13.097	0.645	13.382	0.595
5	8.920	0.336	8.985	0.383

Table 13: Three-gluon vertex in asymmetric kinematic configuration,  $V = 8^4$   $\beta = 2.2$

$p^2$	$G_{fc}^{(3)sym}(p^2)$	$\delta G_{fc}^{(3)sym}(p^2)$	$G_{bc}^{(3)sym}(p^2)$	$\delta G_{bc}^{(3)sym}(p^2)$
2	21.099	1.212	20.483	1.148
4	2.494	0.185	2.512	0.189

Table 14: Three-gluon vertex in symmetric kinematic configuration,  $V = 8^4$   $\beta = 2.2$

$SU(2)$ ,  $V = 8^4$  and  $\beta = 2.3$ , 100 Monte-Carlo configurations  $\times$  100 gauge fixings

Two point functions

$p^2$	$F_{fc}^{(2)}(p^2)$	$\delta F_{fc}^{(2)}(p^2)$	$F_{bc}^{(2)}(p^2)$	$\delta F_{bc}^{(2)}(p^2)$
1	3.742	0.109	3.656	0.084
2	1.569	0.043	1.544	0.032
3	0.945	0.022	0.941	0.019
4 $p^{[4]=16}$	0.755	0.021	0.751	0.016
4 $p^{[4]=4}$	0.669	0.015	0.663	0.013
5	0.562	0.009	0.564	0.009

Table 15: Ghost propagator,  $V = 8^4$   $\beta = 2.3$

$p^2$	$G_{fc}^{(2)}(p^2)$	$\delta G_{fc}^{(2)}(p^2)$	$G_{bc}^{(2)}(p^2)$	$\delta G_{bc}^{(2)}(p^2)$
0	35.140	1.555	34.659	1.597
1	9.7073	0.107	9.839	0.156
2	4.487	0.054	4.503	0.055
3	2.668	0.027	2.652	0.018
4 $p^{[4]=16}$	1.934	0.022	1.919	0.020
4 $p^{[4]=4}$	1.811	0.016	1.823	0.015
5	1.414	0.014	1.414	0.014

Table 16: Gluon propagator,  $V = 8^4$   $\beta = 2.3$

Three point functions

$p^2$	$G_{fc}^{(3)\text{asym}}(p^2)$	$\delta G_{fc}^{(3)\text{asym}}(p^2)$	$G_{bc}^{(3)\text{asym}}(p^2)$	$\delta G_{bc}^{(3)\text{asym}}(p^2)$
1	614.254	42.333	641.328	47.008
2	165.962	7.456	161.354	7.730
3	65.054	2.786	63.734	2.734
4 $p^{[4]=16}$	33.456	3.787	32.685	3.535
4 $p^{[4]=4}$	33.770	1.801	35.883	2.099
5	20.471	0.9744	19.994	1.168

Table 17: Three-gluon vertex in asymmetric kinematic configuration,  $V = 8^4$   $\beta = 2.3$

$p^2$	$G_{fc}^{(3)\text{sym}}(p^2)$	$\delta G_{fc}^{(3)\text{sym}}(p^2)$	$G_{bc}^{(3)\text{sym}}(p^2)$	$\delta G_{bc}^{(3)\text{sym}}(p^2)$
2	26.483	1.260	26.774	1.280
4	2.249	0.105	2.424	0.104

Table 18: Three-gluon vertex in symmetric kinematic configuration,  $V = 8^4$   $\beta = 2.3$

$SU(2)$ ,  $V = 16^4$  and  $\beta = 2.1$ , 100 Monte-Carlo configurations  $\times$  100 gauge fixings

Two point functions

$p^2$	$F_{fc}^{(2)}(p^2)$	$\delta F_{fc}^{(2)}(p^2)$	$F_{bc}^{(2)}(p^2)$	$\delta F_{bc}^{(2)}(p^2)$
1	23.930	0.304	22.615	0.226
2	10.538	0.200	10.188	0.113
3	6.372	0.159	6.257	0.087
4 $p^{[4]=16}$	4.551	0.116	4.405	0.103
4 $p^{[4]=4}$	4.489	0.119	4.421	0.062
5	3.437	0.086	3.344	0.053

Table 19: Ghost propagator,  $V = 16^4$   $\beta = 2.1$

$p^2$	$G_{fc}^{(2)}(p^2)$	$\delta G_{fc}^{(2)}(p^2)$	$G_{bc}^{(2)}(p^2)$	$\delta G_{bc}^{(2)}(p^2)$
0	8.485	0.440	8.309	0.251
1	8.182	0.122	7.871	0.102
2	7.186	0.073	7.022	0.071
3	6.359	0.037	6.385	0.037
4 $p^{[4]=16}$	6.058	0.091	5.874	0.086
4 $p^{[4]=4}$	5.710	0.081	5.669	0.067
5	5.161	0.029	5.195	0.026

Table 20: Gluon propagator,  $V = 16^4$   $\beta = 2.1$

Three point functions

$p^2$	$G_{fc}^{(3)\text{sym}}(p^2)$	$\delta G_{fc}^{(3)\text{sym}}(p^2)$	$G_{bc}^{(3)\text{sym}}(p^2)$	$\delta G_{bc}^{(3)\text{sym}}(p^2)$
2	19.861	3.809	27.689	5.911
4	14.769	2.586	18.952	2.937

Table 21: Three-gluon vertex in symmetric kinematic configuration,  $V = 16^4$   $\beta = 2.1$

$SU(2)$ ,  $V = 16^4$  and  $\beta = 2.2$ , 100 Monte-Carlo configurations  $\times$  100 gauge fixings

Two point functions

$p^2$	$F_{fc}^{(2)}(p^2)$	$\delta F_{fc}^{(2)}(p^2)$	$F_{bc}^{(2)}(p^2)$	$\delta F_{bc}^{(2)}(p^2)$
1	20.867	0.376	20.406	0.392
2	9.151	0.145	9.070	0.192
3	5.499	0.083	5.460	0.085
4 $p^{[4]}=16$	3.861	0.095	3.838	0.082
4 $p^{[4]}=4$	3.803	0.067	3.819	0.068
5	2.929	0.041	2.979	0.067

Table 22: Ghost propagator,  $V = 16^4$   $\beta = 2.2$

$p^2$	$G_{fc}^{(2)}(p^2)$	$\delta G_{fc}^{(2)}(p^2)$	$G_{bc}^{(2)}(p^2)$	$\delta G_{bc}^{(2)}(p^2)$
0	14.473	0.676	15.380	0.635
1	12.614	0.255	12.330	0.184
2	10.564	0.066	10.531	0.097
3	8.813	0.081	8.769	0.061
4 $p^{[4]}=16$	7.760	0.162	7.577	0.089
4 $p^{[4]}=4$	7.447	0.052	7.429	0.073
5	6.393	0.052	6.395	0.044

Table 23: Gluon propagator,  $V = 16^4$   $\beta = 2.2$

Three point functions

$p^2$	$G_{fc}^{(3)asym}(p^2)$	$\delta G_{fc}^{(3)asym}(p^2)$	$G_{bc}^{(3)asym}(p^2)$	$\delta G_{bc}^{(3)asym}(p^2)$
1	136.266	91.211	115.376	53.064
2	93.912	39.689	90.432	26.263
3	84.119	17.125	81.880	17.916
4 $p^{[4]}=16$	101.745	17.120	99.140	18.988
4 $p^{[4]}=4$	78.176	15.640	63.382	14.634
5	51.954	7.666	56.088	8.017

Table 24: Three-gluon vertex in asymmetric kinematic configuration,  $V = 16^4$   $\beta = 2.2$

$p^2$	$G_{fc}^{(3)sym}(p^2)$	$\delta G_{fc}^{(3)sym}(p^2)$	$G_{bc}^{(3)sym}(p^2)$	$\delta G_{bc}^{(3)sym}(p^2)$
2	93.161	11.297	87.022	10.680
4	34.756	7.434	37.655	5.797

Table 25: Three-gluon vertex in symmetric kinematic configuration,  $V = 16^4$   $\beta = 2.2$

$SU(2)$ ,  $V = 16^4$  and  $\beta = 2.3$ , 100 Monte-Carlo configurations  $\times$  100 gauge fixings

Two point functions

$p^2$	$F_{fc}^{(2)}(p^2)$	$\delta F_{fc}^{(2)}(p^2)$	$F_{bc}^{(2)}(p^2)$	$\delta F_{bc}^{(2)}(p^2)$
1	18.326	0.297	17.157	0.172
2	7.993	0.150	7.645	0.089
3	4.824	0.086	4.684	0.060
4 $p^{[4]=16}$	3.431	0.053	3.317	0.052
4 $p^{[4]=4}$	3.364	0.054	3.338	0.048
5	2.581	0.025	2.533	0.036

Table 26: Ghost propagator,  $V = 16^4$   $\beta = 2.3$

$p^2$	$G_{fc}^{(2)}(p^2)$	$\delta G_{fc}^{(2)}(p^2)$	$G_{bc}^{(2)}(p^2)$	$\delta G_{bc}^{(2)}(p^2)$
0	32.705	1.063	31.557	0.721
1	21.940	0.444	21.616	0.385
2	15.007	0.122	15.206	0.166
3	11.400	0.107	11.235	0.116
4 $p^{[4]=16}$	8.848	0.190	8.882	0.108
4 $p^{[4]=4}$	8.904	0.118	8.782	0.099
5	7.057	0.062	6.978	0.045

Table 27: Gluon propagator,  $V = 16^4$   $\beta = 2.3$

Three point functions

$p^2$	$G_{fc}^{(3)\text{asym}}(p^2)$	$\delta G_{fc}^{(3)\text{asym}}(p^2)$	$G_{bc}^{(3)\text{asym}}(p^2)$	$\delta G_{bc}^{(3)\text{asym}}(p^2)$
1	1192.828	250.675	779.501	204.768
2	566.632	39.161	505.435	46.025
3	402.454	32.415	388.260	26.754
4 $p^{[4]=16}$	272.205	35.491	242.150	30.928
4 $p^{[4]=4}$	239.204	35.152	241.295	25.467
5	174.210	14.126	169.739	10.825
6	130.209	7.523	125.733	7.563

Table 28: Three-gluon vertex in asymmetric kinematic configuration,  $V = 16^4$   $\beta = 2.3$

$p^2$	$G_{fc}^{(3)\text{sym}}(p^2)$	$\delta G_{fc}^{(3)\text{sym}}(p^2)$	$G_{bc}^{(3)\text{sym}}(p^2)$	$\delta G_{bc}^{(3)\text{sym}}(p^2)$
2	283.901	15.417	313.824	15.595
4	81.695	5.785	72.573	5.787

Table 29: Three-gluon vertex in symmetric kinematic configuration,  $V = 16^4$   $\beta = 2.3$

# References

- [1] V. N. Gribov. Quantization of non-abelian gauge theories. *Nucl. Phys.*, B139:1, 1978.
- [2] L. Giusti, M. L. Paciello, C. Parrinello, S. Petrarca, and B. Taglienti. Problems on lattice gauge fixing. *Int. J. Mod. Phys.*, A16:3487–3534, 2001, hep-lat/0104012.
- [3] M. Semenov-Tyan-Shanskii and V. Franke. All gauge orbits and some gribov copies encompassed by the gribov horizon. *Zap. Nauch. Sem. Leningrad. Otdeleniya Matematicheskogo Instituta im. V. A. Steklova, AN SSSR*, vol. 120:159, 1982. (English translation: New York, Plenum Press 1986).
- [4] G. Dell’Antonio and D. Zwanziger. All gauge orbits and some gribov copies encompassed by the gribov horizon. In *\*Cargese 1989, Proceedings, Probabilistic methods in quantum field theory and quantum gravity\* 107-130. (see HIGH ENERGY PHYSICS INDEX 29 (1991) No. 10571)*.
- [5] Pierre van Baal. More (thoughts on) gribov copies. *Nucl. Phys.*, B369:259–275, 1992.
- [6] Daniel Zwanziger. Critical limit of lattice gauge theory. *Nucl. Phys.*, B378:525–590, 1992.
- [7] Attilio Cucchieri. Gribov copies in the minimal landau gauge: The influence on gluon and ghost propagators. *Nucl. Phys.*, B508:353–370, 1997, hep-lat/9705005.
- [8] T. D. Bakeev, Ernst-Michael Ilgenfritz, V. K. Mitrjushkin, and M. Mueller-Preussker. On practical problems to compute the ghost propagator in su(2) lattice gauge theory. *Phys. Rev.*, D69:074507, 2004, hep-lat/0311041.
- [9] A. Sternbeck, E. M. Ilgenfritz, M. Muller-Preussker, and A. Schiller. The influence of gribov copies on the gluon and ghost propagator. *AIP Conf. Proc.*, 756:284–286, 2005, hep-lat/0412011.
- [10] A. Sternbeck, E. M. Ilgenfritz, M. Muller-Preussker, and A. Schiller. The gluon and ghost propagator and the influence of gribov copies. *Nucl. Phys. Proc. Suppl.*, 140:653–655, 2005, hep-lat/0409125.
- [11] P. J. Silva and O. Oliveira. Gribov copies, lattice qcd and the gluon propagator. *Nucl. Phys.*, B690:177–198, 2004, hep-lat/0403026.
- [12] A. Sternbeck, E. M. Ilgenfritz, M. Mueller-Preussker, and A. Schiller. Towards the infrared limit in su(3) landau gauge lattice gluodynamics. *Phys. Rev.*, D72:014507, 2005, hep-lat/0506007.
- [13] A. Sternbeck, E. M. Ilgenfritz, and M. Mueller-Preussker. Spectral properties of the landau gauge faddeev-popov operator in lattice gluodynamics. 2005, hep-lat/0510109.
- [14] Daniel Zwanziger. Fundamental modular region, boltzmann factor and area law in lattice gauge theory. *Nucl. Phys.*, B412:657–730, 1994.
- [15] Jacques C. R. Bloch, Attilio Cucchieri, Kurt Langfeld, and Tereza Mendes. Propagators and running coupling from su(2) lattice gauge theory. *Nucl. Phys.*, B687:76–100, 2004, hep-lat/0312036.

- [16] J. Fingberg, Urs M. Heller, and F. Karsch. Scaling and asymptotic scaling in the su(2) gauge theory. *Nucl. Phys.*, B392:493–517, 1993, hep-lat/9208012.
- [17] Ph. Boucaud et al. Asymptotic behavior of the ghost propagator in su3 lattice gauge theory. 2005, hep-lat/0506031.
- [18] P. Boucaud, J. P. Leroy, J. Micheli, O. Pene, and C. Roiesnel. Lattice calculation of alpha(s) in momentum scheme. *JHEP*, 10:017, 1998, hep-ph/9810322.
- [19] B. Alles et al.  $\alpha_s$  from the nonperturbatively renormalised lattice three gluon vertex. *Nucl. Phys.*, B502:325–342, 1997, hep-lat/9605033.
- [20] P. Boucaud et al. The strong coupling constant at small momentum as an instanton detector. *JHEP*, 04:005, 2003, hep-ph/0212192.
- [21] D. Becirevic et al. Asymptotic scaling of the gluon propagator on the lattice. *Phys. Rev.*, D61:114508, 2000, hep-ph/9910204.
- [22] Daniel Zwanziger. Non-perturbative faddeev-popov formula and infrared limit of qcd. *Phys. Rev.*, D69:016002, 2004, hep-ph/0303028.
- [23] I. L. Bogolubsky, G. Burgio, M. Muller-Preussker, and V. K. Mitrjushkin. Landau gauge ghost and gluon propagators in su(2) lattice gauge theory: Gribov ambiguity revisited. 2005, hep-lat/0511056.